

MPPT for Photovoltaic Systems with SEPIC Converter Counting Steady-State and Drift Analysis

Mr. Narayan L. Khiste,
Student, Dept. of Electrical engineering,
AISSMS IOIT , Kennedy Road
Pune, India.
e-mail: knarayan92@gmail.com

Mrs. K. S. Gadgil
Asst. Professor, Dept. of Electrical engineering,
AISSMS IOIT, Kennedy Road
Pune, India.
e-mail:krutujagadgil@yahoo.com

Abstract—A versatile voltage-sensor-based most extreme control point following calculation utilizing a variable scaling calculate for a solitary finished essential inductance converter is exhibited. In this strategy, just a voltage divider circuit is utilized to detect the photovoltaic (PV) board voltage. This technique can adequately enhance both transient and steady state execution by shifting the scaling variable as looked at with the settled stride estimate and versatile stride measure with settled scaling component. For sudden change in sunlight based insolation or, on the other hand in start-up, this technique prompts quicker following, though in enduring state, it prompts bring down motions around most extreme control point. The unfaltering state conduct and float marvels are additionally tended to in this paper to decide the following productivity. The obligation cycle is created specifically without utilizing any proportional–integral control circle to improve the control circuit. MATLAB/Simulink is utilized for reproduction thinks about, and a microcontroller is utilized as a computerized stage to actualize the proposed calculation for trial approval. The proposed framework is actualized what's more, tried effectively on a PV board in the research center.

Keywords—Adaptive, drift phenomena, maximum power point following (MPPT), photovoltaic (PV), single-finished essential inductance converter (SEPIC), voltage sensor.

I. INTRODUCTION

The rapid increase in the demand for electricity and the recent change in the environmental conditions such as global warming led to a need for a new source of energy that is cheaper and sustainable with less carbon emissions. Solar energy has offered promising results in the quest of finding the solution to the problem. The harnessing of solar energy using PV modules comes with its own problems that arise from the change in insolation conditions. These changes in insolation conditions severely affect the efficiency and output power of the PV modules. A great deal of research has been done to improve the efficiency of the PV modules. A number of methods of how to track the maximum power point of a PV module have been proposed to solve the problem of efficiency and products using these methods have been manufactured and are now commercially available for consumers. As the market is now flooded with varieties of these MPPT that are meant to improve the efficiency of PV modules under various insolation conditions it is not known how many of these can really deliver on their

promise under a variety of field conditions. This research then looks at how a different type of converter affects the output power of the module and also investigates if the MPPT that are said to be highly efficient and do track the true maximum power point under the various conditions. A MPPT is used for extracting the maximum power from the solar PV module and transferring that power to the load. A SEPIC converter serves the purpose of transferring maximum power from the solar PV module to the load.

II. PHOTOVOLTAIC OPERATION

A solar cell basically is a p-n semiconductor junction. When exposed to light, a dc current is generated. The generated current varies linearly with the solar irradiance. The standard equivalent circuit of the PV cell is shown in Figure 1. The basic equation that describes the (I-V) characteristics of the PV model is given by the following equation:

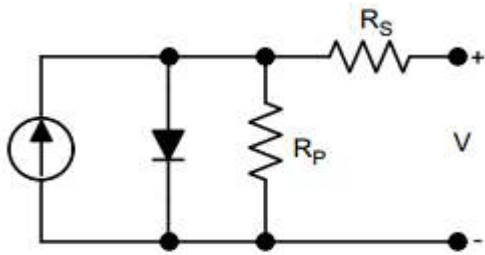


Figure 1. Simple PV model

Single PV output current:

$$I = I_{ph} - I_0 \times \left(e^{\frac{q \times (V + I \times R_s)}{n \times k \times T}} - 1 \right) - \frac{V + I \times R_s}{R_p} \quad (1)$$

R_p is parallel leakage resistance and is normally substantial, $> 100k\omega$ in most current PV cells. This segment can be disregarded in numerous applications aside from low light conditions.

Current through the diode is represented by

$$I_0 \times \left(e^{\frac{q \times (V + I \times R_s)}{n \times k \times T}} - 1 \right) \quad (2)$$

Where:

I_s = Diode saturation current

q = Electron charge (1.6×10^{-19} C)

k = Boltzmann constant (1.38×10^{-23} J/K)

n = Ideality factor (from 1 to 2)

T = Temperature ($^{\circ}$ K)

The value $\frac{q}{n \times k \times T}$ is weak function of $\ln(\text{irradiance})$. This most likely is a change in the ideality factor as the irradiance changes.

The parameters usually given in PV data sheets are:

V_{OC} = Open circuit output voltage

I_{SC} = Short circuit output current

V_{MP} = Maximum power output voltage

I_{MP} = Maximum power output current

III. Different MPPT techniques

There are different techniques used to track the maximum power point. Few of the most popular techniques are:

- 1) Perturb and Observe (hill climbing method)
- 2) Incremental Conductance method
- 3) Fractional short circuit current
- 4) Fractional open circuit voltage
- 5) Neural networks
- 6) Fuzzy logic

The choice of the algorithm depends on the time complexity the algorithm takes to track the MPP, implementation cost and the ease of implementation.

3.1 Perturb & Observe

Perturb & Observe (P&O) is the simplest method. In this we use only one sensor, that is the voltage sensor, to sense the PV array voltage and so the cost of implementation is less and hence easy to implement. The time complexity of this algorithm is very less but on reaching very close to the MPP it doesn't stop at the MPP and keeps on perturbing on both the directions. When this happens the algorithm has reached very close to the MPP and we can set an appropriate error limit or can use a wait function which ends up increasing the time complexity of the algorithm.

However the method does not take account of the rapid change of irradiation level (due to which MPPT changes) and considers it as a change in MPP due to perturbation and ends up calculating the wrong MPP. To avoid this problem we can use incremental conductance method.

3.2 Incremental Conductance

Incremental conductance method uses two voltage and current sensors to sense the output voltage and current of the PV array.

At MPP the slope of the PV curve is 0.

$$(dP/dV)_{MPP} = d(VI/dV) \quad (3)$$

$$0 = I + (dP/dV)_{MPP} \quad (4)$$

$$(dI/dV)_{MPP} = -I/V \quad (5)$$

The left hand side is the instantaneous conductance of the solar panel. When this instantaneous conductance

equals the conductance of the solar then MPP is reached. Here we are sensing both the voltage and current simultaneously. Hence the error due to change in irradiance is eliminated. However the complexity and the cost of implementation increase.

As we go down the list of algorithms the complexity and the cost of implementation goes on increasing which may be suitable for a highly complicated system. This is the reason that Perturb and Observe and Incremental Conductance method are the most widely used algorithms. Owing to its simplicity of implementation we have chosen the Perturb & Observe algorithm for our study among the two.

3.3 Fractional open circuit voltage

The near linear relationship between V_{MPP} and V_{OC} of the PV array, under varying irradiance and temperature levels, has given rise to the fractional V_{OC} method.

$$V_{MPP} = k_1 V_{OC} \quad (6)$$

where k_1 is a constant of proportionality. Since k_1 is dependent on the characteristics of the PV array being used, it usually has to be computed beforehand by empirically determining V_{MPP} and V_{OC} for the specific PV array at different irradiance and temperature levels. The factor k_1 has been reported to be between 0.71 and 0.78. Once k_1 is known, V_{MPP} can be computed with V_{OC} measured periodically by momentarily shutting down the power converter. However, this incurs some disadvantages, including temporary loss of power.

3.4 Fractional short circuit current

Fractional I_{SC} results from the fact that, under varying atmospheric conditions, I_{MPP} is approximately linearly related to the I_{SC} of the PV array.

$$I_{MPP} = k_2 I_{SC} \quad (7)$$

where k_2 is a proportionality constant. Just like in the fractional V_{OC} technique, k_2 has to be determined according to the PV array in use. The constant k_2 is generally found to be between 0.78 and 0.92. Measuring I_{SC} during operation is problematic. An

additional switch usually has to be added to the power converter to periodically short the PV array so that I_{SC} can be measured using a current sensor

3.5 Fuzzy Logic Control

Microcontrollers have made using fuzzy logic control popular for MPPT over last decade. Fuzzy logic controllers have the advantages of working with imprecise inputs, not needing an accurate mathematical model, and handling nonlinearity.

3.6 Neural Network

Another technique of implementing MPPT which are also well adapted for microcontrollers is neural networks. Neural networks commonly have three layers: input, hidden, and output layers. The number nodes in each layer vary and are user-dependent. The input variables can be PV array parameters like V_{OC} and I_{SC} , atmospheric data like irradiance and temperature, or any combination of these. The output is usually one or several reference signals like a duty cycle signal used to drive the power converter to operate at or close to the MPP.

IV. METHODOLOGY

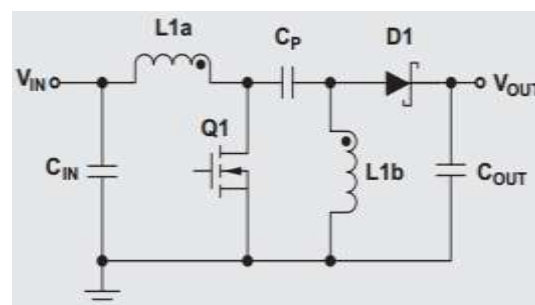


Figure 2. Simple circuit diagram of SEPIC converter

4.1 Basic operation

Figure 2 demonstrates a basic circuit diagram of a SEPIC converter, comprising of an input capacitor, C_{IN} ; an output capacitor, C_{OUT} ; coupled inductors L_{1a} and L_{1b} ; an AC coupling capacitor, C_P ; a power FET, Q_1 ; and a diode, D_1 . Figure 2 shows the SEPIC operating in continuous conduction mode (CCM).

To understand the voltages at the various circuit nodes, it is important to analyze the circuit at DC when Q_1 is off and not switching. During steady-state CCM, pulse-width modulation (PWM) operation,

and neglecting ripple voltage, capacitor C_p is charged to the input voltage, V_{in} .

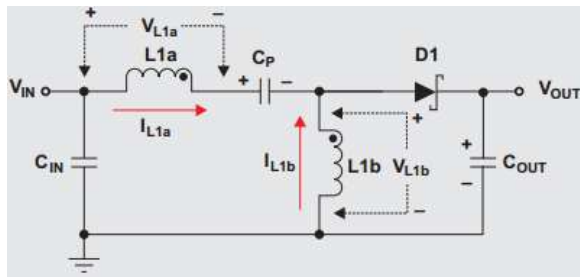


Figure 3. When Q1 is off in SEPIC converter

When Q_1 is off, the voltage across L_{1b} must be V_{out} . Since C_{in} is charged to V_{in} , the voltage across Q_1 when Q_1 is off is $V_{in} + V_{out}$, so the voltage across L_{1a} is V_{out} .

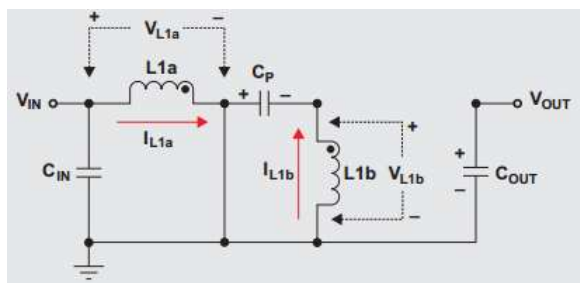


Figure 4. When Q1 is on in SEPIC converter

When Q_1 is on, capacitor C_p , charged to V_{in} , is connected in parallel with L_{1b} , so the voltage across L_{1b} is $-V_{in}$. When Q_1 is on, energy is being stored in L_{1a} from the input and in L_{1b} from C_p .

When Q_1 turns off, L_{1a} 's current continues to flow through C_p and D_1 , and into C_{out} and the load. Both C_{out} and C_p get recharged so that they can provide the load current and charge L_{1b} , respectively, when Q_1 turns back on.

Case 1: For Resistive Load

Utilizing information and yield voltage connection for SEPIC (i.e., $V_o = (D/(1 - D))V_{PV}$), the effectiveness of the converter can be communicated as

$$\eta = \frac{V_o I_o}{V_{PV} I_{PV}} = \left(\frac{V_o}{V_{PV}} \right)^2 \frac{R_{eq}}{R_L} = \left(\frac{D}{1-D} \right)^2 \frac{R_{eq}}{R_L} \quad (8)$$

where V_{PV} and I_{PV} are the PV voltage and current, separately. The comparable info resistance R_{eq} of the converter can be gotten from (1) as takes after:

$$R_{eq} = \eta \left(\frac{1 - D}{D} \right)^2 R_L. \quad (9)$$

By utilizing (9), the yield control from the PV module, which is input energy to the converter, is given by

$$P = \frac{V_{PV}^2}{R_{eq}} = \frac{V_{PV}^2}{\eta R_L} \left(\frac{D}{1 - D} \right)^2 \quad (10)$$

Both P and square foundation of energy (P^*) have the greatest incentive at a similar obligation cycle (D). By considering the square base of energy (P^*) to get a target work for following the most extreme power, the accompanying condition can be gotten:

$$P^* = \sqrt{P} = \frac{V_{PV}}{\sqrt{\eta R_L}} \left(\frac{D}{1 - D} \right) \quad (11)$$

At MPP, the incline of the P^* bend is zero (i.e., $dP^*/dD = 0$), and it can be assessed as

$$\frac{dP^*}{dD} = \left(V_{PV} \frac{1}{(1 - D)^2} + \frac{D}{1 - D} \frac{dV_{PV}}{dD} \right) \frac{1}{\sqrt{\eta R_L}} = 0 \quad (12)$$

$$\frac{dP^*}{dD} = \left(\frac{V_{PV} dD + D(1 - D) dV_{PV}}{(1 - D)^2 dD} \right) \frac{1}{\sqrt{\eta R_L}} = 0 \quad (13)$$

By evaluating dP^*/dD using (13) at MPP, the objective function Q can be obtained as follows:

$$Q = D(1 - D) dV_{PV} + V_{PV} dD \begin{cases} = 0, & \text{at MPP} \\ > 0, & \text{on left of MPP} \\ < 0, & \text{on right of MPP} \end{cases} \quad (14)$$

Consequently, contingent upon the indication of Q, the MPPT calculation chooses whether to increment or decline the obligation cycle, and the comparing Q–D attributes

Case 2: Versatile Voltage-Sensor-Based MPPT with Variable Scaling Factor

In this paper, a versatile voltage-sensor-based MPPT with variable scaling component is proposed to lessen the following time what's more, power misfortune in consistent state. The present and past cycle estimations of PV voltage and obligation cycle of the converter are indicated by $V_{PV(k)}$, $V_{PV(k-1)}$, $D_{(k)}$, and $D_{(k-1)}$,

individually. The adjustments in the voltage and obligation cycle from the present emphasis to the following cycle are characterized as takes after:

$$dV_{PV} = V_{PV(k)} - V_{PV(k-1)} \quad (15)$$

$$dD = d1 - Dk \quad (16)$$

The area of the working point is chosen by assessing Q what's more, contingent upon the indication of Q; the obligation cycle is augmented or, then again decremented by ΔD as given in (10). On the off chance that Q is certain, then the obligation cycle is augmented by ΔD, and if Q is negative, then the obligation cycle is decremented by ΔD. As ΔD is straight forwardly utilized in altering the obligation cycle, the controller is basic and simple to actualize with a microcontroller. In this manner,

$$D_{(k+1)} = D_{(k)} \pm \Delta D \quad (17)$$

The value of Q is large in start-up and during insolation change, whereas it is small in the steady state. Thus, a fixed scaling factor cannot satisfy the requirement of MPPT controller in different conditions. Hence, in this proposed algorithm, two different scaling factors M1 and M2 are considered to optimally vary the perturbation step size ΔD, which has been defined as a linear function of Q by

$$\Delta D = M_i Q \quad (18)$$

The scaling component Mi (i = 1, 2) assumes a critical part in a versatile MPPT strategy; hence, it ought to be picked wisely to build the pinnacle control following productivity. The scaling factor M1 is lessened the following time in startup what's more, for an expansive change in insolation. The scaling component M2 is lessened the power misfortune in the relentless state. In this way, the proposed versatile MPPT technique enhances both the transient furthermore, relentless state execution.

The scaling variable either M1 or M2 is produced ΔD relying upon the estimation of Q concerning a predefined limit estimation of the goal work, i.e., Qth, as appeared in the pseudocode of the calculation. By considering an upper restrict (ΔDmax) of 10% and a lower confine (ΔDmin) of 0.5% to bother step measure (ΔD), the scaling variables M1 and M2 ought to comply (19) and (20), individually, with a specific end

goal to ensure the union of the MPPT calculation. The estimation of ΔD will fluctuate amongst ΔDmin and ΔDmax, as given in (14). In this manner,

$$M_1 Q \leq \Delta D_{max} \quad (19)$$

$$M_2 Q \geq \Delta D_{min} \quad (20)$$

$$\Delta D = \begin{cases} \Delta D_{max}, & \text{if } \Delta D > \Delta D_{max} \\ \Delta D, & \text{if } \Delta D_{max} \leq \Delta D \leq \Delta D_{min} \\ \Delta D_{min}, & \text{if } \Delta D < \Delta D_{min}. \end{cases} \quad (21)$$

Case 3: Unfaltering State Analysis

The development of the working point on Q–D attributes also, the comparing point on P–V qualities is appeared in Fig. 4. Accept that the working point amid (k–3)Ta time interim is at point a . As Q > 0 at point a, the calculation builds the obligation cycle, and thus, the working guide pushes toward point bamid (k–)Ta time interim. At point b, the algorithm again builds the obligation cycle as Q > 0, furthermore, the working point moves to point c. additionally at point c, the calculation builds the obligation cycle since Q > 0, and consequently, the working point moves to point d amid kTa time interim. At point d, as Q < 0, the algorithm decreases the obligation cycle, and henceforth, the working point moves back to point c . Again at point c, as Q > 0, the calculation makes the working indicate move to point d by expanding the obligation cycle. Accordingly, in enduring state, the working point moves in two levels, coming about in power misfortune diminishment contrasted and P&O and IncCond since, if there should be an occurrence of P&O [20], the working point moves in three levels.

V. MATLAB/SIMULATION

5.1 Conventional Method:

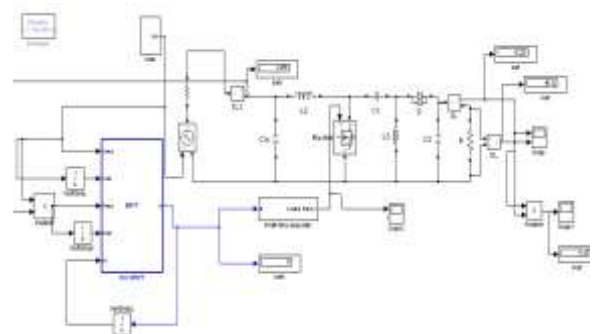


Figure 4. Conventional Method Simulation diagram

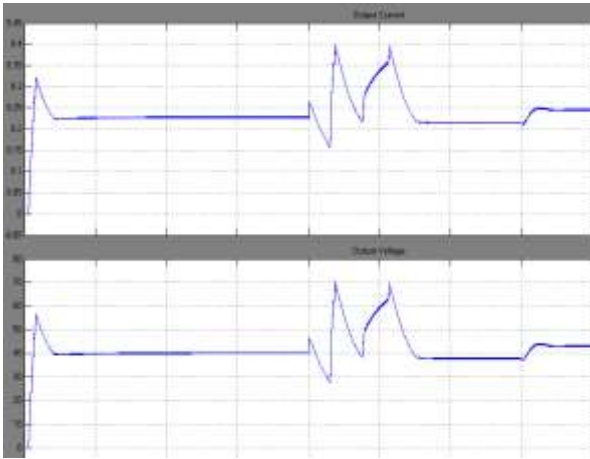


Figure 5. Output voltage and Output current waveform

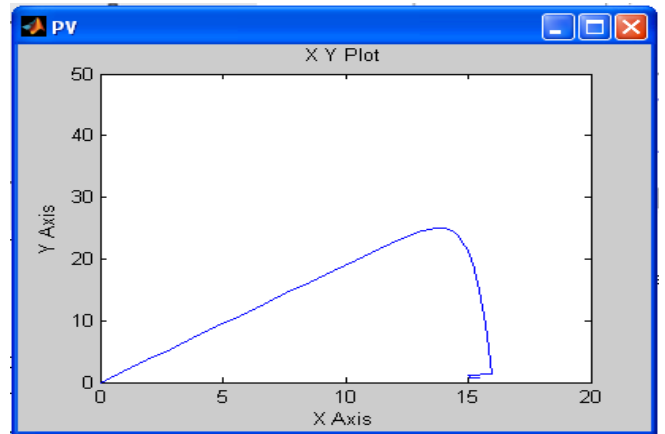


Figure 8. Photovoltaic Voltage waveform

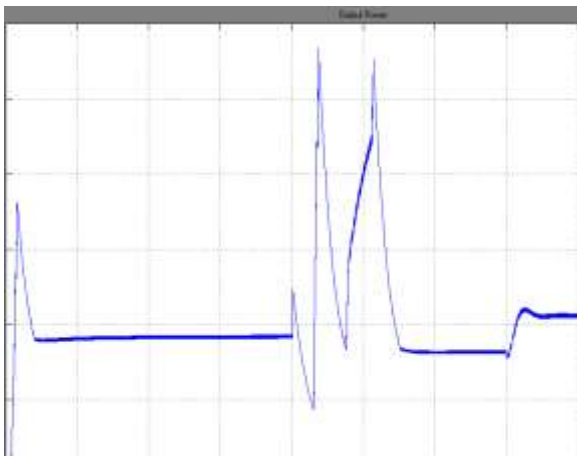


Figure 6. Output Power waveform

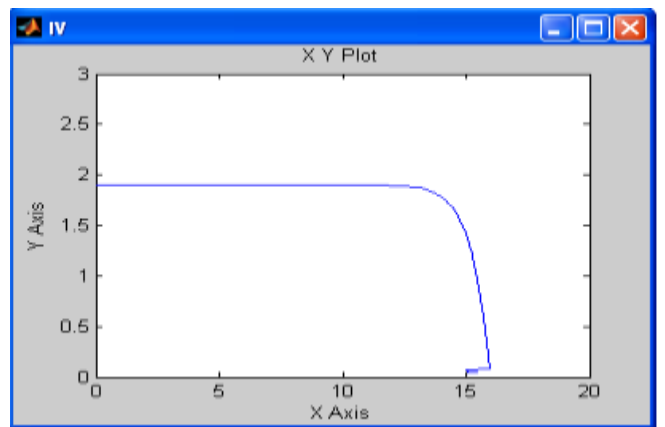


Figure 9. Photovoltaic Current waveform

5.2 Proposed Method:

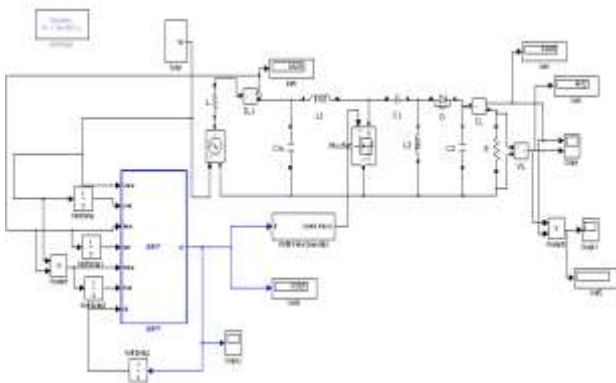


Figure 7. Simulation diagram MPPT based SEPIC converter

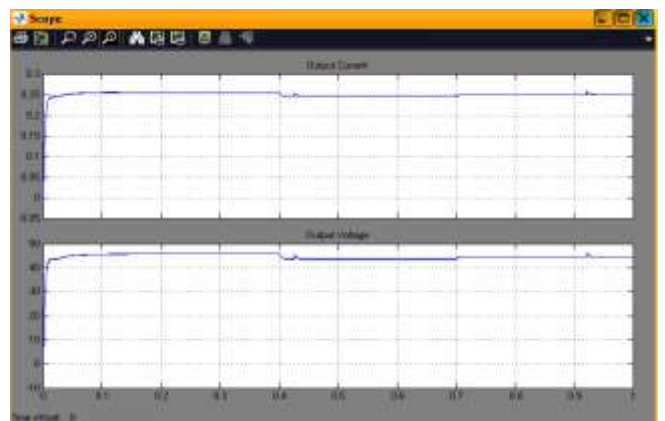


Figure 10. Output Voltage and Current waveform



Figure 11. Output Power waveform

Algorithm for Proposed Method:

function d1 = MPPT(Vnew,Vold,Inew,Iold,Pnew,Pold,dD)

% V=Input Voltage; v1=New Voltage; I=Input current;

a=New current;d=Calculated duty cycle

Vnew = 16;

Inew = 1.9;

d1 = 0.5;

$D_k = \frac{dD - (dD + 0.5)(V_{new}/V_{old})}{V_{new}/V_{old}}$;

dV=Vnew-Vold;

dP=Pnew-Pold;

% dI=Inew-Iold;

% Pnew=Vnew*Inew;

% Pold=Vold*Iold;

if(dP/dD==0)

 dD=d1-Dk;

else if(dP/dD>0)

 % p & O Method

 if(dP>0)

 if(dV>0)

 d1=d1+Dk;

 else

 d1=d1-Dk;

 end

 else

 if(dV<0)

 d1=d1-Dk;

 else

 d1=d1+Dk;

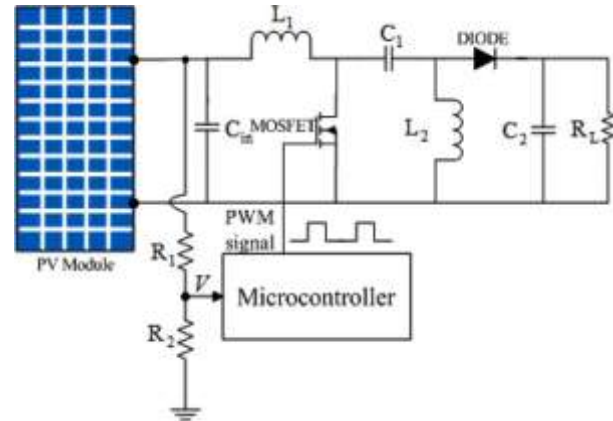
 end

 end

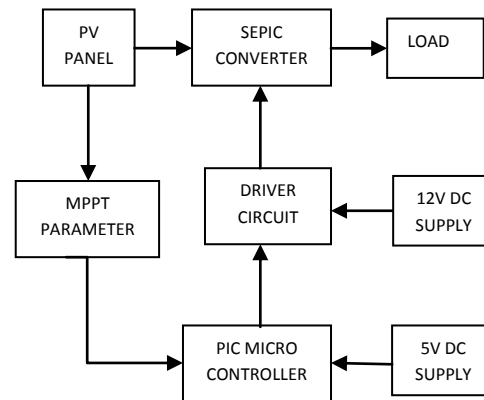
 d1=Dk;

end
 d1=Dk+1;
 end

VI. HARDWARE APPROACH



6.1. Block Diagram:



6.2. Hardware Circuit Diagram:

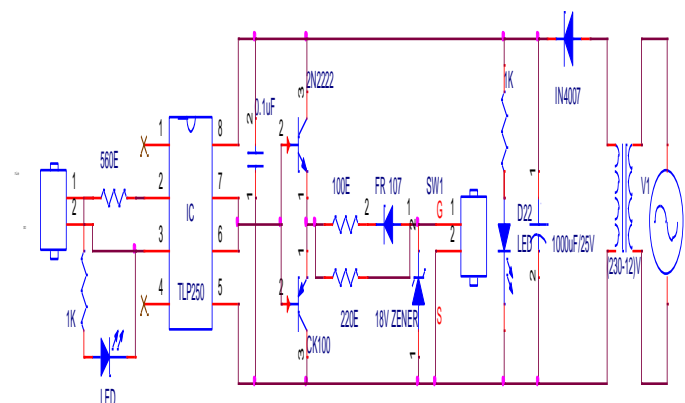


Figure 7. Driver Circuit Diagram

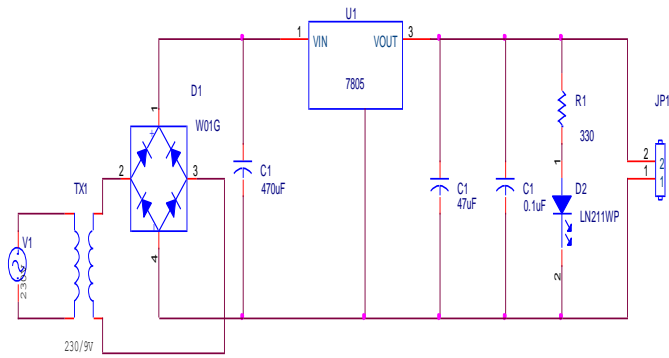


Figure 12. Power Supply Circuit for PIC16F877A

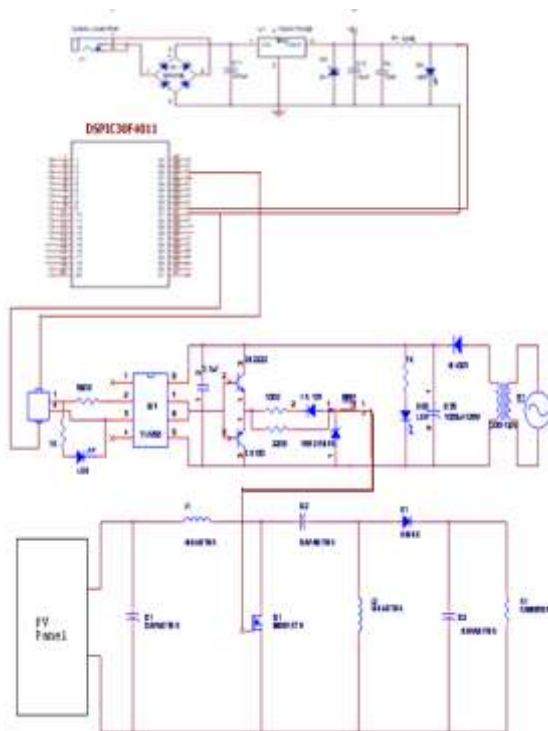


Figure 13. Full Circuit Diagram

Duty cycle calculation:

For a SEPIC converter operating in a CCM, the duty cycle is given by

$$D = \frac{V_{OUT} + V_D}{V_{IN} + V_{OUT} + V_D} \tag{22}$$

V_D is the forward voltage drop of the diode D1. The maximum duty cycle is:

$$D_{max} = \frac{V_{OUT} + V_D}{V_{IN (min)} + V_{OUT} + V_D} \tag{23}$$

Output voltage:

$$V_{out} = \frac{DV_{in}}{1 - D} \tag{24}$$



Figure 14. Hardware image

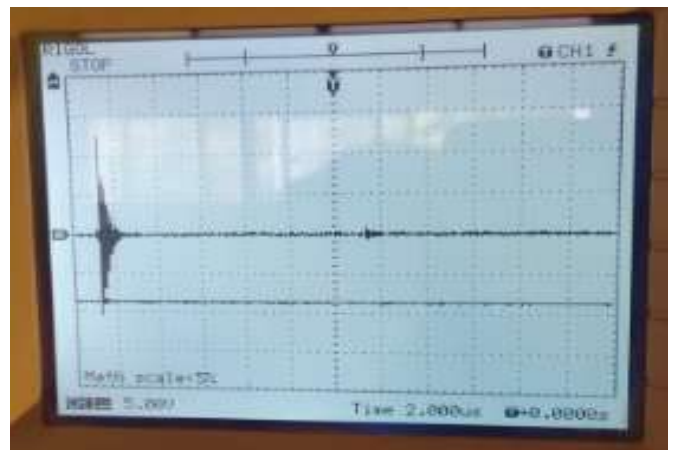


Figure 15. Output volatage image

VII CONCLUSION

In this paper, MPPT algorithm with variable scaling factor by considering direct duty cycle control method for SEPIC converter has been implemented. The proposed system is designed, and the functionality of MPPT control has been proved. The simulation and experimental results prove that the proposed system is able to track the maximum power from the PV module; moreover, the steady-state two-level operation and the drift-free phenomena are the merits of this tracking algorithm. Hence, this method improves the efficiency of the PV system and reduces power loss in steady state. From the results obtained, it is noticed that, with a well-designed system, including a proper converter and an efficient MPPT algorithm, the MPPT can be developed with less complexity and reduced cost.

REFERENCES

- [1] M. G. Villalva, J. R. Gazoli, and E. R. Filho, "Comprehensive approach to modeling and simulation of photovoltaic arrays," *IEEE Trans. Power Electron.*, vol. 24, no. 5, pp. 1198–1208, May 2009.
- [2] J. H. R. Enslin, M. S. Wolf, D. B. Snyman, and W. Swiegers, "Integrated photovoltaic maximum power point tracking converter," *IEEE Trans. Ind. Electron.*, vol. 44, no. 6, pp. 769–773, Dec. 1997.
- [3] M. A. S. Masoum, H. Dehbonei, and E. F. Fuchs, "Theoretical and experimental analyses of photovoltaic systems with voltage and current-based maximum power-point tracking," *IEEE Trans. Energy Convers.*, vol. 17, no. 4, pp. 514–522, Dec. 2002.
- [4] W. Xiao and W. G. Dunford, "A modified adaptive hill climbing MPPT method for photovoltaic power systems," in *Proc. IEEE PESC*, 2004, pp. 1957–1963.
- [5] D. Sera, R. Teodorescu, J. Hantschel, and M. Knoll, "Optimized maximum power point tracker for fast-changing environmental conditions," *IEEE Trans. Ind. Electron.*, vol. 55, no. 7, pp. 2629–2637, Jul. 2008.
- [6] K. L. Lian, J. H. Jhang, and I. S. Tian, "A maximum power point tracking method based on perturb-and-observe combined with particle swarm optimization," *IEEE J. Photovoltaics*, vol. 4, no. 2, pp. 626–633, Mar. 2014.
- [7] F. Liu, S. Duan, B. Liu, and Y. Kang, "A variable step size INC MPPT method for PV systems," *IEEE Trans. Ind. Electron.*, vol. 55, no. 7, pp. 2622–2628, Jul. 2008.
- [8] A. Safari and S. Mekhilef, "Simulation and hardware implementation of incremental conductance MPPT with direct control method using Cuk converter," *IEEE Trans. Ind. Electron.*, vol. 58, no. 4, pp. 1154–1161, Apr. 2011.
- [9] K. S. Tey and S. Mekhilef, "Modified incremental conductance algorithm for photovoltaic system under partial shading conditions and load variation," *IEEE Trans. Ind. Electron.*, vol. 61, no. 10, pp. 5384–5392, Oct. 2014.
- [10] Q. Mei, M. Shan, L. Liu, and J. M. Guerrero, "A novel improved variable step-size incremental-resistance MPPT method for PV systems," *IEEE Trans. Ind. Electron.*, vol. 58, no. 6, pp. 2427–2434, Jun. 2011.
- [11] T. Esumi, J. W. Kimball, P. T. Krein, P. L. Chapman, and P. Midya, "Dynamic maximum power point tracking of photovoltaic arrays using ripple correlation control," *IEEE Trans. Power Electron.*, vol. 21, no. 5, pp. 1282–1291, Sep. 2006.
- [12] T. Wu, C. Chang, and Y. Chen, "A fuzzy-logic-controlled single-stage converter for PV-powered lighting system applications," *IEEE Trans. Ind. Electron.*, vol. 47, no. 2, pp. 287–296, Apr. 2000.
- [13] Syafaruddin, E. Karatepe, and T. Hiyama, "Artificial neural network-polar coordinated fuzzy controller based maximum power point tracking control under partially shaded conditions," *IET Renew. Power Gener.*, vol. 3, no. 2, pp. 239–253, Jul. 2009.
- [14] K. Ishaque and Z. Salam, "A deterministic particle swarm optimization maximum power point tracker for photovoltaic system under partial shading condition," *IEEE Trans. Ind. Electron.*, vol. 60, no. 8, pp. 3195–3206, Aug. 2013.
- [15] E. Bianconi *et al.*, "A fast current-based MPPT technique employing sliding mode control," *IEEE Trans. Ind. Electron.*, vol. 60, no. 3, pp. 1168–1178, Mar. 2013.